UDK: 623.462:621.375.826, 629.7.018
COSATI: 19-02, 20-05, 16-04

Normal force coefficient C_z determination and flow visualization on the fin of the laser guided bomb model in the T-38 wind tunnel

Slavica Ristić, PhD (Eng)[1)]
Dijana Dmljanović, BSc (Eng)[1)]

In this paper, aerodynamic test results and boundary layer flow visualization on the fin of laser guided bomb model are presented. The test was performed in the T-*38* wind tunnel. The influence of the fin position relative to the conic top of the model on aerodynamic characteristics of the fin was analyzed. Analysis was performed for three Mach numbers M_∞=0.5, 0.8, 0.9, and four fin deflections δ=0, 5, 10, 15°. Analysis of the influence of the two fin positions on the aerodynamic characteristics of the fin is presented by normal force coefficient and it shows that there is significant result deviation. Normal force on the fin was measured by internal three-component strain gauge balance. Aerodynamic results obtained were associated with the flow visualization results, which were performed by oil emulsion method. The presented images of flow visualization show changes of streamlines depending on the fin position and confirm the results of the aerodynamic measurement.

Key words: **guided bomb, laser guided, fin, aerodynamic characteristics, aerodynamic coefficients, normal force, boundary layer, flow visualization.**

Used symbols

M_∞	– Nominal Mach number in *T-38* wind tunnel test section
v	– Free flow velocity, (m/s)
d	– Referent model diameter, (m)
P_o	– Stagnation pressure in the *T-38* wind tunnel test section, (bar)
α_n	– Nominal total angle of attack of the model,(°)
α	– Total angle of attack of the model, (°)
δ	– Deflection angle of the fin, (°)
δ_4	– Deflection angle of the measured fin, (°)
t	– Wind tunnel run time, (s)
C_z	– Normal force coefficient of the fin
RSN	– Run sequence number
POZPRS	– Model parameter
LGB	– Laser guided bomb
F.S.	– Full scale
RT	– Fin reference point
X_B	– Axis identification (body axes system of fin)
Y_B	– Axis identification (body axes system of fin)
Z_B	– Axis identification (body axes system of fin)
∞	– Index for free flow parameters

Introduction

AERODYNAMIC tests of the *LGB* model in the subsonic and transonic speed ranges were performed in *T-38* wind tunnel of the Military Technical Institute. The range of the model angles of attack was –12° to +15°. The purpose of the test was to determine aerodynamic coefficients of the model, especially of the fin.

Two different model configurations were tested, the basic model configuration and modified model configuration with ring mounted in front of the fin section.

For the basic model configuration, the experimentally obtained curves for the normal force coefficient of the fin, $C_z=f(\alpha,\delta_4)$ on Mach number M_∞=0.8 are smooth with the clearly visible stall effect. In the tests on Mach number M_∞=0.9, the curves $C_z=f(\alpha,\delta_4)$ are not smooth and there is the stall effect on smaller angles of attack.

Assuming that the shape of the curves of the fin aerodynamic coefficients as functions of the angle of attack are caused by conic nose influence, the modified model configuration was tested.

Boundary layer flow visualization on the model was included in the test programme to get more information about the flow, especially on the fin. Test results deviation can be analyzed using images of flow visualization. Boundary layer flow visualization was performed on Mach numbers M_∞=0.5, 0.8, 0.9 and because of that the oil emulsion method was the best choice with the broadest opportunities.

In this paper, besides the *LGB* model, *T-38* wind tunnel, instrumentation, data recording, data reduction, visualization method and the experiment are described.

Comparative analysis of the aerodynamic coefficient results and flow visualization images was performed. The summary of the investigation results are given in the conclusion.

Exsperiment

Model

The *LGB* model consists of three-stage cylindrical body with a conic nose, control fin section and wing section *[1]*.

Control section comprises four fins, which can be

[1)] Military Technical Institute (VTI), Ratka Resanovića 1, 11132 Belgrade, SERBIA

maintained in discreet positions around individual hinge axes. They can be fixed on seven defined positions in δ range of ±15°, with step of 5° relative to the model longitudinal axis. Fig.1 shows the control fin. The measuring fin is the one that is horizontal (position 4 in Fig.2) for zero roll angle of the model.

The rear section of the model consists of wing holders and wings mounted on the perimeter of the model body. The angles between the consecutive wings are 90°. The wing section has no possibility to deflect. Model is in the so-called *"+"* position for zero roll angle.

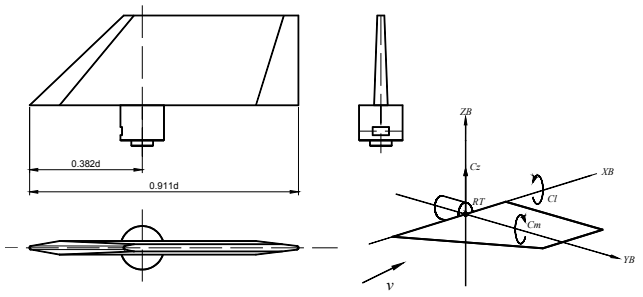

Figure 1. Control fin and body axis coordinate system of the measuring fin

Type of the model construction is modular and it enables testing of different model configurations. Fig.2 shows control fin section as part of the basic (A) and modified (B) model configurations, with the fin positions.

During the experiment, it was necessary to define different parameters to describe the tested model configuration. The appropriate number of rings ensures the necessary model length. Parameter *POZPRS* describes which rings are mounted. Each ring is designated with a number: 1, 2 or 3.

The value of the parameter *POZPRS* is 23 for the basic model configuration. The position of the control fin section relative to the model top is 1.074*d*.

The value of the parameter *POZPRS* is 123 for the modified model configuration. The ring with 0.877*d* diameter and 0.314*d* width was mounted in front of the control fin section. The ring was mounted in this model configuration to determine the influence of the conic nose on the fin aerodynamic characteristics. Position of the control fin section relative to the model top is 1.388*d*.

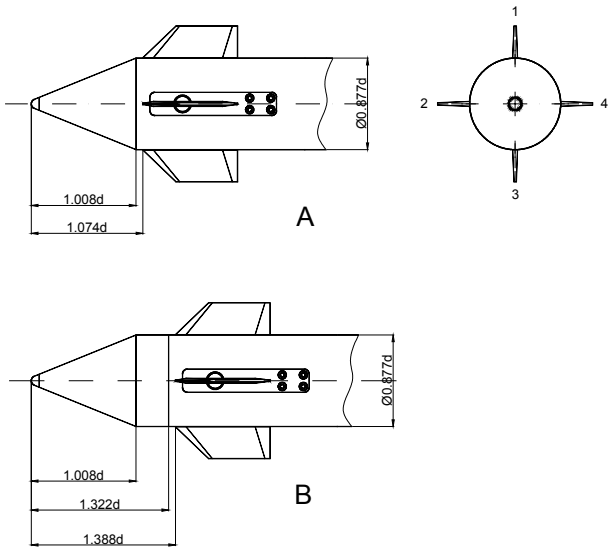

Figure 2. Control fin section in the basic (A) and modified (B) *LGB* model configurations with the given fin position

Figure 3. Basic configuration of the *LGB* model in the *T-38* wind tunnel test section

LGB model was designed, manufactured, checked and assembled in the workshop of the Military Technical Institute.

The model was supported in the test section by sting mounted on a pitch-and-roll mechanism in the *T-38* wind tunnel. Fig.3 shows the basic configuration of the *LGB* model in the *T-38* wind tunnel test section.

T-38 wind tunnel

T-38 wind tunnel in the *VTI* is a blowdown pressurized wind tunnel with 1.5 x 1.5 m square test section [2]. Mach numbers in the range of 0.2 to 4.0 can be achieved in the test section with Reynolds numbers up to 115 million per meter. Mach number can be set and regulated to within ±0.3% of its nominal value.

Stagnation pressure in the test section can be maintained between 1.1 and 15 bar depending on Mach number, and it can be regulated with accuracy of up to ±0.3% of its nominal value. Run times are in the range 6 s to 60 s depending on Mach number and stagnation pressure.

The model is supported in the test section by sting mounted on a pitch-and-roll mechanism. It is possible to achieve the desired aerodynamic angles in the pitch angle range –12° to +21° and in the roll angle range 0° to 360°. The facility supports both continuous and step-by-step model movements during measurement.

Instrumentation and data recording

Absolute and differential transducers of Mensor and Druck type were used for measuring the pressures. The ranges of these transducers are different. The nonlinearity and hysteresis of the transducers of these types are typically 0.02 % F.S.

Resolvers were mounted in the pitch-and-roll mechanism of the model support. The resolution of the pitching angle resolver is ±0.05° and of the rolling angle resolver ±0.25°.

The *VTI40A* internal six-component strain gauge balance was used for measuring the aerodynamic forces and moments acting on the model. The balance was mounted on a sting of 48 mm diameter. The accuracy of this balance is 0.3% F.S. The balance was calibrated before the test [3].

Three-component strain gauge balance was used for measuring the normal force, bending moment and hinge moment acting on the horizontal fin 4. The accuracy of this balance is 0.2% F.S. The balance was calibrated before the test [4].

One-component strain gauge roll element was used for measuring the hinge moment acting on the horizontal fin 2. The accuracy of the used element is 0.2% F.S. The element was calibrated before the test [5].

The data acquisition system comprised *Teledyne* 64 channels "front-end" controlled by *PC Compaq* computer.

The appropriate gains and filters of appropriate cut frequencies were set on all analog channels.

A 16-bit resolution A/D converter digitized the data from all analog channels. All channels were sampled with the same 200 samples/s rate.

The digitized data were received on a *Compaq AlphaServer DS20E* computer and stored on a disk for later reduction.

Data reduction

Data reduction was performed after each run, using the standard *T38 Application Software package* in use with the wind tunnel facility. It was done in several stages, i.e.:

1. Reading raw data, normalizing and converting them to standard format;
2. Determining the flow parameters;
3. Determining the model position;
4. Determining the aerodynamic coefficients.

A specialized software module was used to perform each data reduction stage.

Axis system, used for presenting the results in this paper, is the body axes system of horizontal fin 4, (see Fig.1). The origin of this axis system is in the chosen fin reference point. The X_B, Y_B, Z_B axes are parallel to the appropriate axes of the three-component balance axis system, which is tied to the model. The X_B axis is parallel to the model longitudinal axis and positive towards the tail of the model. The Z_B axis is parallel to the model symmetry plane and positive in the upward direction. The orientation of the Y_B axis is to the left side of the model and completes the left-hand side coordinate system. The angle of attack α is the angle between X_B axis and the projection of the air velocity vector on the X_BZ_B plane. The angle of attack α is positive when the projection of the air velocity on Z_B axis is positive.

The angle of fin deflection δ is the angle between the fin symmetry plane and the X_BY_B plane. Deflection δ of the control fin is defined as positive if it is clockwise when looking outwards along the individual hinge axis.

Flow visualization

Boundary layer flow visualization based on oil emulsions was chosen. This method has a very long tradition in experimental aerodynamics [8-13]. It was necessary to prepare the tested model during fabrication, i.e. to blacken the model surface to provide a maximum visibility of the flow visualization. Visualization was an additional requirement in the test programme and changing of the model or the model set up in the wind tunnel was impractical. Thus, visualization process was started without previous preparations of the model although it was known that the flow visualization would be less visible on the photos recorded. Three types of pigments were used in experiments:

1. Powder of titanium dioxide TiO_2,
2. Powder of titanium dioxide TiO_2 with aniline violet paint supplement,
3. Graphite.

Paraphine oil and oleic acid were the base of all oil emulsions.

Flow visualization was preformed on all model surfaces. Emulsions were discreetly spread as dots by a little brush on the right half of the model and continually by sponge on the left half of the model [13].

Two model angles of attack were chosen, α_n=0° and α_n=6°. Model was set in the desired position before the airflow started. During wind tunnel run and after it the model remained in that position. The roll angle of the model was zero during all wind tunnel runs.

Total wind tunnel run time was about 25 s. There was enough time for oil emulsions flow image to be developed. Visualization was performed on Mach numbers M_∞= 0.5, 0.8 and 0.9.

The wind tunnel was opened up after each run to take a photo of the model. Aerodynamic forces and moments acting on the model were not measured during the flow visualization test. Primary measuring system was turned on to control the flow parameters [13].

Results and discussion

Analysis of aerodynamic forces and moments measurement results

Figures 4-7 show aerodynamic results in the form of graphs. Figures 4 and 5 show normal force coefficients C_z of the fin as functions of the fin angle of attack α and the fin deflection δ_4 at Mach number M_∞=0.8 and 0.9 for basic model configuration. Experimentally obtained curves $C_z=f(\alpha,\delta_4)$ at Mach number M_∞=0.8, shown in Fig.4, are smooth with the clearly visible stall effect. The curves are approximately linear in the range of small angles of attack. Experimental curves $C_z=f(\alpha,\delta_4)$ at Mach number M_∞=0.9, shown in Fig.5, are not smooth and the stall effect is not clearly visible. Stall effect tendency and very variable gradient are present in the whole range of the angles of attack.

Fig.6 shows comparative graphs for the fin normal force coefficient C_z on the fin deflection δ_4=-15° at Mach numbers M_∞=0.5, 0.8 and 0.9 for basic model configuration. Experimentally obtained curves at Mach numbers M_∞=0.5 and 0.8 are smooth, approximately linear in the range of small angles of attack, with clearly visible stall effect on α=10° and α=4°, respectively. Variable gradient and earlier decrease of C_z are observed on experimental curves at Mach number M_∞=0.9.

It is assumed that the flow around the fin is disturbed by conic nose of the model at Mach number M_∞=0.9. A ring was mounted in front of the control fin section to investigate the registered interference effects. The testing of the modified model configuration with maximum fin deflection δ_4=-15° at Mach number M_∞=0.9 was performed.

Fig.7 shows comparative graphs of normal force coefficient C_z for fin deflection δ_4=-15° for the basic and modified model configurations at Mach number M_∞=0.9. Experimentally determined curves show significant mutual deviations. Experimental curve of aerodynamic coefficient C_z of the fin in the modified model configuration is smooth, linear in the range of small angles of attack, with clearly visible stall effect on α=7°.

It is concluded that the flow field disturbances are more visible at higher Mach numbers when the fins are closer to the model top.

Aerodynamic measurements of the forces and moments cannot give all answers about these phenomena. Flow visualization was included in the test programme to get more information about it.

Analysis of the flow visualization results

Flow visualization was performed on three Mach

numbers, M_∞=0.5, 0.8, 0.9 and two *LGB* model configurations, basic and modified. During the visualization test, deflections of the horizontal fins were δ=-15°.

Table 1 gives the survey of the flow visualization part of the experiment. Number of the figure, *RSN*, nominal flow parameters, model parameter *POZPRS* that describe the tested model's configuration, model angle of attack and run time are shown there. Flow visualization photos for the whole *LGB* model are given in reference [13].

To analyze the flow on the horizontal fin, which depends on the fin position relative to the conic nose of the model, photos of flow visualization on the upper surface of the horizontal fin 4 are chosen.

Flow on the fin upper surface for the basic model configuration at Mach number M_∞=0.9 is shown in Fig.8 for α=0.29° and in Fig. 10 for α=7.22°. Flow on the fin upper surface for the basic model configuration at Mach number M_∞=0.8 is shown in Fig. 9 for α=0.42° and in Fig.11 for α=7.07°.

Flow on the fin upper surface for the modified model configuration on Mach number M_∞=0.9 is shown in Fig.12 for α=0.50° and in Fig.13 for α = 7.56°.

Figures 14 and 15 show flow on the fin upper surface for the basic model configuration at Mach number M_∞=0.5 for α=6.76° and α=0.28°.

The analysis of flow images is very complex. In this paper, flow images of the horizontal fin 4 are presented, where normal force coefficient C_z was measured. It should be point out that the flow is three-dimensional and transonic at Mach numbers M_∞=0.8 and 0.9 and subsonic at Mach number M_∞=0.5. The fins are in the zone of influence of the model body and expansion waves that are formed at the ends of the model's conic nose.

Photos in Figures 14 and 15 show the expected boundary layer flow images at Mach number M∞=0.5. Boundary layer flow is laminar. There is a small turning of streamlines towards the fin tip in the part closer to the model body. Strong turning of streamlines exists in the zone of expansion waves. The influence of the model body is observed in the first third of the fin semi-span. In this area, streamlines are almost parallel to the fin chord. The area of flow separation is just on the fin tip for α=0.28° (Fig.14), moving towards the fin root for α=6.76° and covering a larger area (Fig.15). Oil emulsions are accumulated in area of flow separation. This area is quite small in relation to complete fin area and there is no significant influence on the measured normal force coefficient C_z of the fin.

Flow on the fin lower surface is laminar [13]. Oil emulsions visualize streamlines on the fin tip, which pass from its lower to the upper side. This phenomenon is visible in the first third of the fin chord. In this region, turbulent flow zone can be seen on the fin upper side. There is no significant influence on the measured normal force coefficient C_z of the fin. Turbulent flow can be seen in the vicinity of the fin root on the upper surface, where the flow passes through the slot between the body and the fin. Fig.6 shows normal force coefficient C_z of the fin at Mach number M_∞=0.5. It is evidently that C_z on α=6.76° is in the linear part of the diagram with positive gradient.

Figures 9 and 11 show flow images on the fin upper surface at Mach number M_∞=0.8 and angles α=0.42° and α=7.07°, respectively. As expected, the flow images are different, because the model angles of attack α are chosen for different flow regimes. There is a large laminar area (Fig.9) for zero angle of attack. Fig.4 shows coefficient C_z in the linear part of the diagram with positive gradient for α=0.42°. The flow is more complex for α=7.07° (Fig.11). The separation of boundary layer occurs on the leading edge and it is turbulent in the largest part of the fin upper surface. The flow passing from the fin lower side is distinct on the trailing edge and it contributes to decreasing the entire normal force coefficient C_z (see Fig.4).

Figures 8 - 12 show flow images of the fin upper surface at Mach number M_∞=0.9 and zero angle of attack α, for basic and modified model configurations. The results of aerodynamic measurements and flow visualization confirm flow differences. The flow is mainly turbulent for the basic model configuration. There are two zones of flow separation, on the leading edge and on about 50% of the fin chord (see Fig.8). It could be noticed that the stall effect is visible for α=-1° (see Fig.7). The coefficient C_z for α=-1° is in the linear part of the curve with positive gradient for the modified model configuration (see Fig.7). Fig.12 shows that the flow is mainly laminar, except on the leading edge (one third of the fin length from the fin tip) where the local shock wave is observed.

The flow image on the fin upper surface for the modified model configuration at M_∞=0.9 and α=0.50° (see Fig.12) is very similar to the flow image of the fin upper surface for the basic model configuration at M_∞=0.8 and α=0.42° (see Fig.9). Figures show that the flow is mainly laminar and also that the local shock wave is observed on the leading edge.

Normal force coefficient C_z of the fin for the basic model configuration at M_∞=0.8 and α=0.42° has the value of 0.519 (see Fig.6). Normal force coefficient C_z of the fin for the modified model configuration at M_∞=0.9 and α=0.50° has the value of 0.565 (see Fig.7). Similarity of the flow images confirms a small difference between C_z numerical values.

Normal force coefficient C_z of the fin for the basic model configuration at M_∞=0.9 and α=7.22° has the value of 0.594 (see Fig.7). The coefficient C_z for the modified model configuration at M_∞=0.9 and α=7.56° has the value of 0.896 (also see Fig.7). Photos show that the boundary layer flow is laminar for larger part of the fin in the modified model configuration (see Fig.13) than the flow for the fin in the basic model configuration (see Fig.10). The difference between the flow images confirms the difference in C_z numerical values.

Detailed analysis of the flow requires a variation of a large number of parameters during the experiment, and the possibility to utilize and compare the effects of at least two visualization methods. These would make it easier to interpret the experimental images, to identify all phenomena and to eliminate the shortcomings of each method.

Table 1. Survey of the flow visualization on the *LGB* model fin

No of figure	RSN	M_∞	P_0, bar	POZPRS	α, °	t, s
8	43	0.9	2.3	23	0.29	25
9	44	0.8	2.3	23	0.42	25
10	45	0.9	2.3	23	7.22	25
11	46	0.8	2.3	23	7.07	25
12	47	0.9	2.3	123	0.50	25
13	48	0.9	2.3	123	7.56	25
14	49	0.5	2.5	23	6.76	25
15	50	0.5	2.5	23	0.28	25

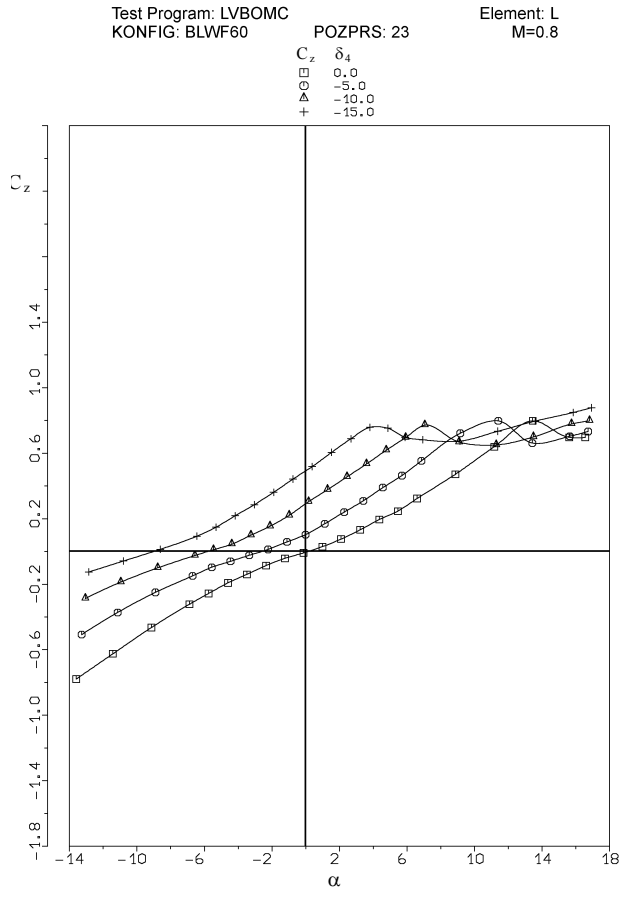

Figure 4. Normal force coefficient $C_z=f(\alpha,\delta_4)$ of the fin for the basic model configuration at M_∞=0.8

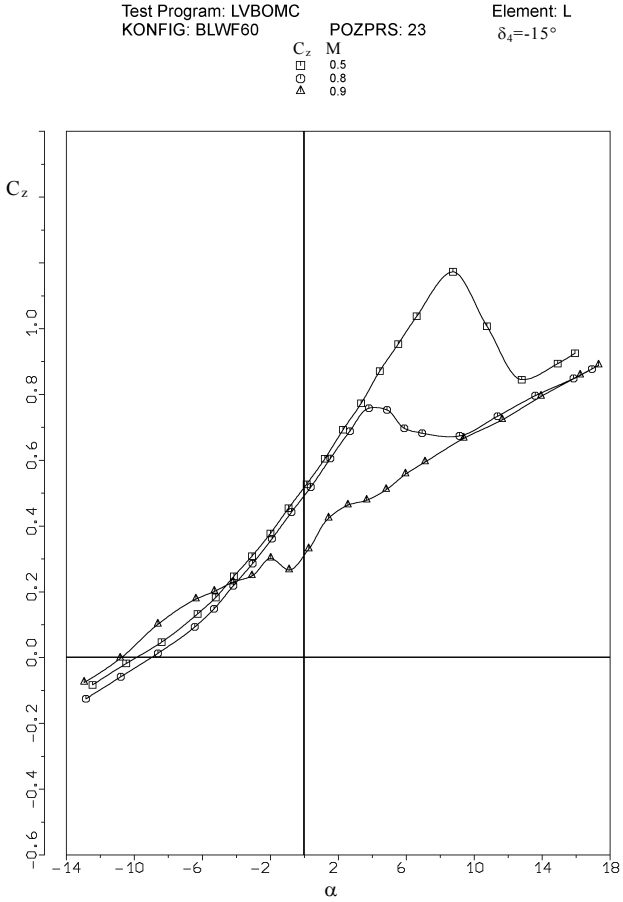

Figure 6. Normal force coefficient $C_z=f(\alpha, M_\infty)$ of the fin with δ_4=-15° deflection for the basic model configuration

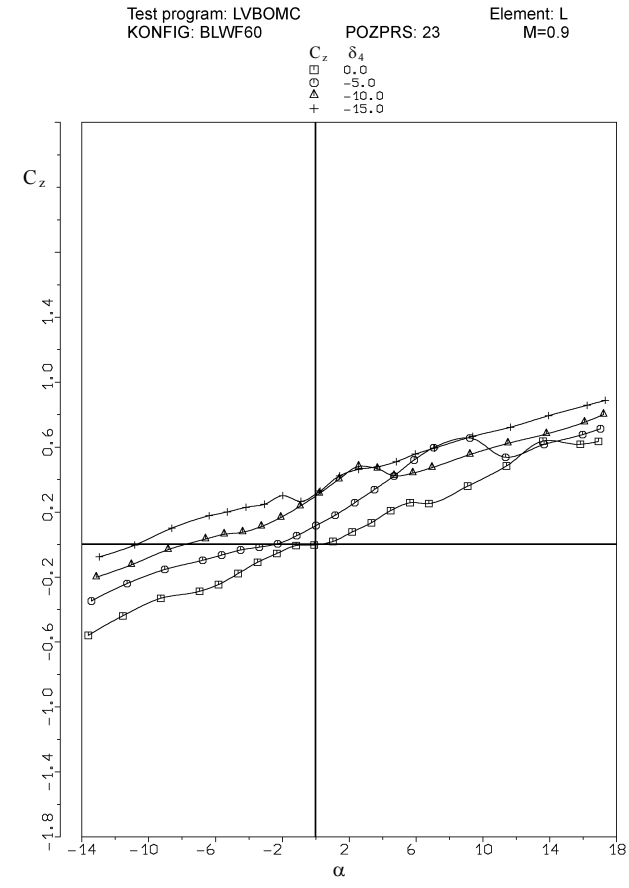

Figure 5. Normal force coefficient $C_z=f(\alpha,\delta_4)$ of the fin for the basic model configuration at M_∞=0.9

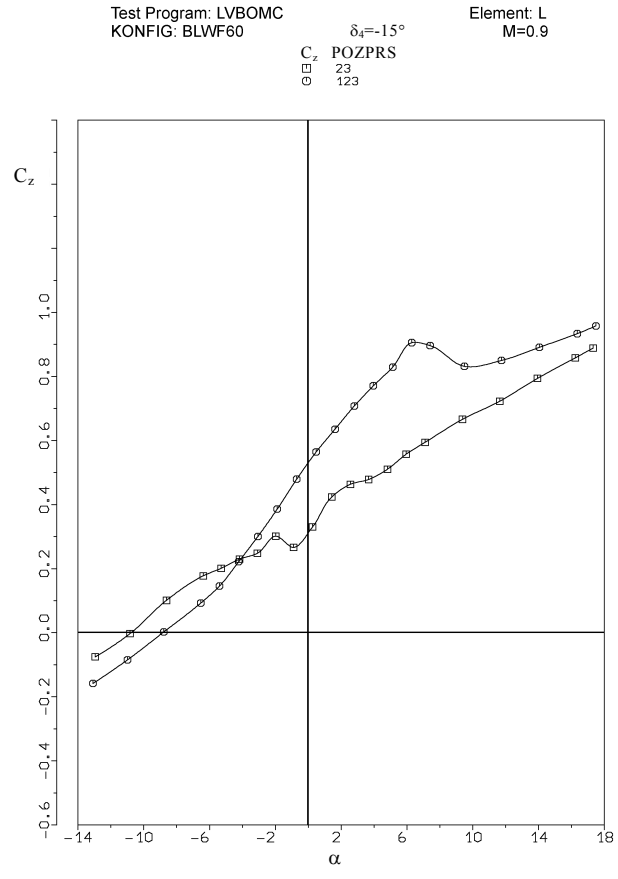

Figure 7. Normal force coefficient $C_z=f(\alpha)$ of the fin with δ_4=-15° deflection for the two model configurations at M_∞=0.9

Figure 8. Flow on the fin upper surface, *RSN*=43

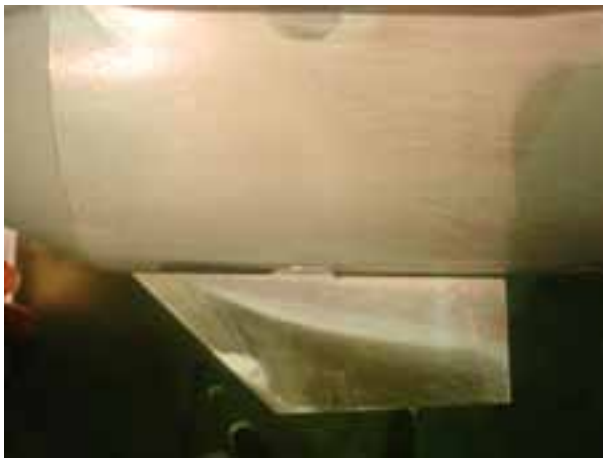

Figure 9. Flow on the fin upper surface, *RSN*=44

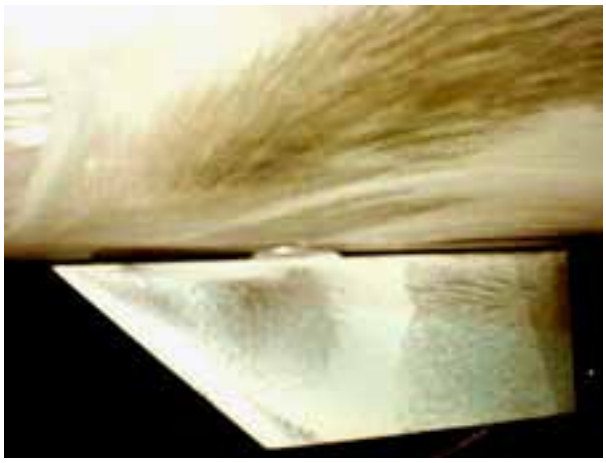

Figure 10. Flow on the fin upper surface, *RSN*=45

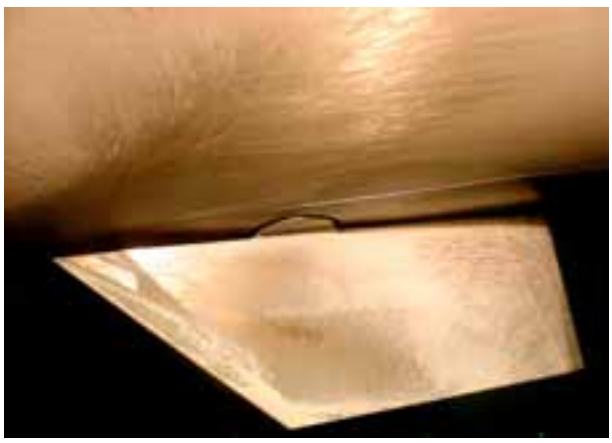

Figure 11. Flow on the fin upper surface, *RSN*=46

Figure 12. Flow on the fin upper surface, *RSN*=47

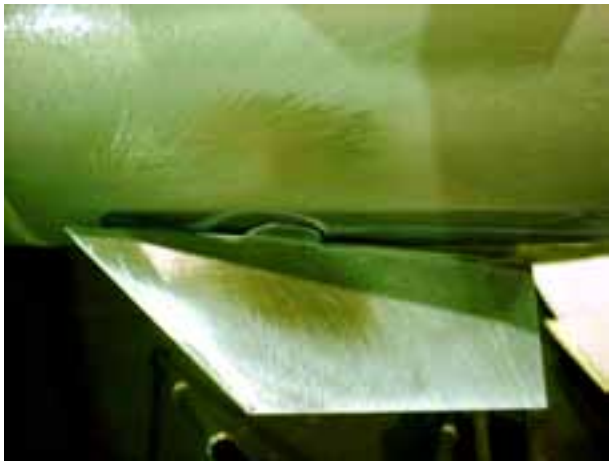

Figure 13. Flow on the fin upper surface, *RSN*=48

Figure 14. Flow on the fin upper surface, *RSN*=49

Figure 15. Flow on the fin upper surface, *RSN*=50

Conclusion

The testing in the *T-38* wind tunnel enabled determining the aerodynamic coefficients of the *LGB* model. Aerodynamic forces and moments acting on the model were measured by internal six-component strain gauge balance. Normal force, bending moment and hinge moment acting on the horizontal fin 4 were measured by three-component strain gauge balance. In this paper, the obtained values of the normal force coefficients C_z on the horizontal fin 4 for different model configurations are considered. It was shown that the character of the experimentally obtained curves $C_z=f(\alpha,\delta_4)$ at Mach number M_∞= 0.9 deviate from the character of curves at Mach number M_∞= 0.8 for the basic model configuration. Deviations are reflected in the variable gradient, non linearity in the range of small angles of attack and earlier lift decreasing.

It was assumed that the deviations of the fin aerodynamic coefficients are the result of the influence of the conic nose, i.e. of the fin section position. A ring mounted between the conic nose and the fin section partly eliminated the flow disturbances. The modified model configuration with δ=-15° fin deflection was tested at Mach number M_∞= 0.9. The experimentally obtained curve $C_z=f(\alpha)$ has approximately linear gradient in the range of small angles of attack and clearly visible stall effect. Curve of the fin normal force coefficient became more similar to the expected form.

The minimal distance between the fin section and the model top that does not produce C_z decrease on small angles of attack can be determined by the ring width variation in future tests. It would be very interesting to test the *LGB* model with other forms of nose (for e.g. *ogival*) and determine their influence on the fin aerodynamic coefficients.

Boundary layer flow visualization using oil emulsion method confirms the results of aerodynamic measurement. Flow images that were recorded under the condition of C_z decreasing show that the flow on the fin upper surface is very complex and mainly turbulent. The area of flow separation is very close to the fin leading edge. A large part of the fin is within the expansion waves zone, which is formed at the ends of the conic nose. More precise and complete flow images could be obtained if *Schlieren* method was included in the test programme. Flow is three-dimensional and complex, and additional testing in transonic speed range using *Schlieren* method is planned.

Cotemporary numerical methods enabled flow simulation around the entire model. Numerical flow image of the fin surface can be compared with the flow visualization image. It is planned to include some numerical method in the additional model testing.

References

[1] DAMLJANOVIĆ,D.: *Ispitivanje modifikovanog modela laserski vođene bombe na Mahovim brojevima 0.5 do 0.9 u aerotunelu T-38*, Vojnotehnički institut, Beograd

[2] ELFSTROM,G.M., MEDVED,B.: *The Yugoslav 1.5m Trisonic Blowdown Wind Tunnel*, AIAA Paper 86-0746-CP

[3] JANJIKOPANJI,G.: *Baždarenje aerovage VTI40A*, Vojnotehnički institut, Beograd

[4] MARINKOVSK,D.I., AMLJANOVIĆ,D.D.: P*roračun i baždarenje trokomponentne aerovage na krmilu modela laserski vođene bombe*, Vojnotehnički institut, Beograd

[5] MARINKOVSKI,D., DAMLJANOVIĆ,D.: *Proračun i baždarenje davača šarnirnog momenta na krmilu modela laserski vođene bombe*, Vojnotehnički institut, Beograd

[6] MARZKIRICH,W.: *Flow visualization*, Academic Press, New York, 1977.

[7] YANG ,W.J.: *Flow visualization* III proc. of 3. International Symposium, An Arbor MI, 1983, Hemisphere, New York, 1985.

[8] RISTIĆ,S.: *Flow Visualization Technics in wind tunnels*, VTI VJ 1996, skripta

[9] RISTIĆ,S.: *Vizualizacija strujanja u aerodinamičkim tunelima*, Glasnik RV i PVO, 1990, 1, 16-24.

[10] RISTIĆ,S.: *Pregled metoda za vizualizaciju strujanja u aerodinamičkim tunelima, kumnti*, VTI VJ, 1999.

[11] WILLEM,C.D.L., PAGENDARM,H.G., FRITS,H.P.T., WALTER,B.: *Visual Simulation of Experimental Oil-Flow Visualization by Spot Noise Images from Numerical Flow Simulation*, 2001.

[12] RISTIĆ,S., VITIĆ,A., MATIĆ,D.: *Vizualizacija i numerička simulacija oko prednjeg dela modela torpeda*, 29. Hipnef 2004, Zbornik radova, str.267-273

[13] RISTIĆ,S.: *Vizualizacija strujanja oko modela laserski vođene bombe u aerotunelu T-38 uljanim premazima,* VTI, interni V3 izveštaj, 2004.

Received: 15.03.2004.:

Određivanje koeficijenta normalne sile C_z i vizualizacija strujanja na krmilu modela laserski vođene bombe u aerotunelu T-38

U radu su prikazani rezultati aerodinamičkih ispitivanja i vizualizacija strujanja u graničnom sloju na krmilu modela laserski vođene bombe. Ispitivanje je izvršeno u aerotunelu T-38. Analiziran je uticaj položaja krmila u odnosu na konus tela na aerodinamičke karakteristike krmila za tri Mahova broja M_∞=0.5, 0.8 i 0.9 i četiri otklona krmila δ=0, 5, 10, 15°. Analiza uticaja konusa na aerodinamičke karakteristike krmila je data preko koeficijenta normalne sile za dva položaja krmila u odnosu na konus i pokazuje da postoji bitno odstupanje rezultata. Rezultati merenja normalne sile na krmilu pomoću trokomponentne aerovage povezani su sa rezultatima vizualizacije strujanja metodom uljnih premaza. Priložene fotografije vizualizacije strujanja ilustruju promene strujnih linija na krmilu modela u zavisnosti od položaja krmila i potvrđuju rezultate aerodinamičkih merenja.

Ključne reči: **laserska vođena bomba, krmilo, aerodinamičke karakteristike, aerodinamički koeficijenti, normalna sila, granični sloj, vizualizacija strujanja.**

Определение коэффициента нормального усилия C_z и визуализация потока на киле модели бомбы с лазерным управлением в аэродинамической трубе Т-38

В настоящей работе показаны результаты аэродинамических испытываний и визуализация потока в пограничном слое на киле модели бомбы с лазерным управлением, а испытывание проведено в аэродинамической трубе Т-38. Тоже сделан анализ влияния положения киля по отношению ко конусу тела на аэродинамические характеристики киля для трёх значений числа Маха M_∞=0.5. 0.8 и 0.9 для четырёх отклонений киля δ=0, 5, 10, 15°. Анализ влияния конуса на аэродинамические характеристики киля проведён через коэффициент нормального усилия для двух положений киля по отношению ко конусу и показывает существование значительного и существенного склонения результатов. Результаты измерения нормального усилия на киле при помощи весов из трёх составляющих связаны со результатами визуализации потока методом масляных плёнок эмульсии. Присоединённые фотографии визуализации потока иллюстрируют изменения линий тока на киле модели в зависимости от положения киля и потверждают результаты аэродинамических измерений.

Ключевые слова: **лазерное управляемая бомба, киль, аэродинамические характеристики, аэродинамические коэффициенты, нормальное усилие, пограничный слой, визуализация потока.**

Détermination du coefficient de la force normale Cz et visualisation du courant chez l'ailette d'équilibrage de la bombe guidée par laser dans la soufflerie aérodynamique T-38

Les résultats des essais aérodynamiques et la visualisation du courant dans la couche limite chez l'ailette d'équilibrage d'une bombe guidée par laser sont présentés dans ce papier. Les essais ont été réalisés dans la soufflerie aérodynamique T-38.On a analysé l'influence de la position de l'ailette d'équilibrage par rapport au cône du corps quant aux caractéristiques dynamiques de l'ailette pour trois nombres de Mach: M=0.5, 0.8, 0.9 et pour quatre déviations de l'ailette: δ=0, 5, 10, 15º. Analyse de l'influence du cône sur les propriétés dynamiques de l'ailette d'équilibrage est donnée à l'aide du coefficient de la force normale pour deux positions de l'ailette par rapport au cône et démontre qu'il y a un changement important du résultat. Les résultats du mesurement de la force normale sur l'ailette d'équilibrage au moyen d'une balance aérienne à trois composantes sont en liaison avec les résultats de la visualisation du courant effectuée par la méthode d'émulsion d'huile. Les photos présentées de la visualisation du courant illustrent les changements des lignes du courant sur le modèle de l'ailette d'équilibrage selon sa position et confirment les résultats des mesurements aérodynamiques .

Mots clés: **laser bombe guidée, ailette d'équilibrage, caractéristiques aérodynamiques, force normale, couche limite, visualisation du courant.**